Identification of putative effector genes across the GWAS Catalog using molecular quantitative trait loci from 68 tissues and cell types

Cong Guo*°, Karsten B. Sieber*°, Jorge Esparza-Gordillo, Mark R. Hurle, Kijoung Song, Astrid J. Yeo, Laura M. Yerges-Armstrong, Toby Johnson, Matthew R. Nelson
*These authors contributed equally to this work
°Please send correspondence to karl.x.guo@gsk.com and karsten.b.sieber@gsk.com

Abstract

Identifying the effector genes from genome-wide association studies (GWAS) is a crucial step towards understanding the biological mechanisms underlying complex traits and diseases. Colocalization of expression and protein quantitative trait loci (eQTL and pQTL, hereafter collectively called “xQTL”) can be effective for mapping associations to genes in many loci. However, existing colocalization methods require full single-variant summary statistics which are often not readily available for many published GWAS or xQTL studies. Here, we present PICCOLO, a method that uses minimum SNP p-values within a locus to determine if pairs of genetic associations are colocalized. This method greatly expands the number of GWAS and xQTL datasets that can be tested for colocalization. We applied PICCOLO to 10,759 genome-wide significant associations across the NHGRI-EBI GWAS Catalog with xQTLs from 28 studies. We identified at least one colocalized gene-xQTL in at least one tissue for 30% of associations, and we pursued multiple lines of evidence to demonstrate that these mappings are biologically meaningful. PICCOLO genes are significantly enriched for biologically relevant tissues, and 4.3-fold enriched for targets of approved drugs.

GWAS have discovered thousands of genetic associations with complex traits and diseases[1]. Most associations cannot be explained by protein coding changes and are expected to be driven by gene regulatory mechanisms[1,2]. Recent studies have shown that xQTLs explain a substantial proportion of complex trait heritability[3,4]. However, it is not enough to demonstrate that a GWAS index SNP is a statistically significant xQTL to conclude that the GWAS and xQTL associations are likely explained by the same underlying functional variant[5]. This requires that the two associations colocalize. A popular colocalization method developed by Giambartolomei *et. al.* determines if two associations are driven by the same signal using full single-variant summary statistics for the genomic region of interest[5]. Already, colocalization analyses have identified candidate effector genes for a variety of complex diseases and traits[6-9]. However, broader application of the colocalization approach is limited by the lack of readily available complete summary statistics from many published GWAS and xQTL studies. Even when the data are available, obtaining and harmonizing results takes significant effort. To overcome the need for full summary statistics and to expand the pool of available GWAS and xQTL studies for colocalization, we developed PICCOLO, a colocalization test using Probabilistic Identification of Causal SNPs (PICS) credible sets that can be estimated using only an index SNP p-value and a linkage disequilibrium reference panel[10]. Using PICCOLO, we colocalized all associations in the NHGRI-EBI GWAS Catalog[11] with eQTLs from The Genotype-Tissue Expression (GTEx) Project[12] along with xQTLs from 27 additional studies[13-38] (Supplementary Table 1).

We created the PICCOLO algorithm by adapting the coloc method[5] to use PICS for estimating causal SNP probabilities. Once causal SNP probabilities for both genetic associations have been estimated, PICCOLO performs a statistical test to evaluate their overlap. In contrast to coloc (Fig. 1a), PICCOLO enables the assessment of colocalization for any two genetic signals

using only published index SNPs (Fig. 1b). PICS estimates the posterior probability of causality for each SNP within a locus using the LD structure from a reference data set and strength of association[10]. Therefore, all that is required to generate posterior probabilities with PICS is the index SNP identifier, the p-value of the index SNP, and the ancestry of the study population. As with coloc, PICCOLO calculates the posterior probability that two genetic associations are either shared (H4) or not shared (H3). In contrast to coloc, PICCOLO does not test the hypotheses of no association for either trait (H1, H2), or both traits (H0).

To evaluate the performance of PICCOLO, we compared PICCOLO with coloc results for 1,490 genome-wide significant loci ($P \leq 5 \times 10^{-8}$) across 13 diverse traits analyzed in UK Biobank[39] (Supplementary Table 2). These loci were tested using coloc and PICCOLO across the 44 GTEx Version 6p eQTL tissues (Supplementary Data 1). Coloc analyses were conducted on full variant-level summary statistics across each locus for both the GWAS and GTEx results. PICCOLO analyses were conducted with just the most significant GWAS and GTEx SNP in each locus. In comparing the two methods, true positives were defined as coloc genes with a posterior probability of H4 ≥ 0.8. Analysis of the PICCOLO parameters identified that PICCOLO H4 ≥ 0.9 and an xQTL $P \leq 1 \times 10^{-5}$ are parameters that provide a strong predictive power for coloc (positive predictive value = 0.89) and reasonable sensitivity (0.52) of coloc results (Fig. 2, Supplementary Figs. 1-3, see methods). We did not observe any impact of allele frequency or credible set size on PICCOLO performance (Supplementary Figs. 4-6). Therefore, differences between PICCOLO and coloc are likely due to limitations of the PICS estimations from the index SNPs.

Since PICCOLO estimates colocalization of genetic associations without complete summary statistics, we used PICCOLO to identify possible causal genes using results available in the NHGRI-EBI GWAS Catalog[11]. We generated PICS probabilities for 23,012 genome-wide significant associations and 23,353 non-genome-wide significant associations. In addition, we generated xQTL PICS probabilities for 44 tissues in GTEx V6p (166,987 unique index SNPs) and 27 other studies (148,259 unique index SNPs)[13-38]. In total, we used xQTLs from 32 broad tissue groups, representing 68 tissues and cell types (Supplementary Table 3).

PICCOLO was then used to assess colocalization of the GWAS and xQTL associations (Supplementary Data 2). Applying our previously selected parameters (H4 ≥ 0.9, xQTL $P \leq 1 \times 10^{-5}$), we found 6,628 (29%) genome-wide significant associations to have ≥ 1 PICCOLO colocalization (Supplementary Data 2). Of the 6,628 associations with PICCOLO colocalizations, GTEx eQTLs uniquely accounted for colocalizations for 2,500 associations (39%), non-GTEx xQTLs accounted for 1,802 associations (27%), and 2,240 (33%) associations were accounted for by both. These results highlight the added value of using index SNPs across additional xQTL sources to map genetic associations to putative effector genes.

Of GWAS loci with PICCOLO colocalizations, 2,730 (62%) colocalized with one gene in one or more cell types (gene-specific loci). Of those, 1,189 (27%) had colocalization with a single gene in a single cell type (gene- and tissue- specific loci, Fig. 3a). These results suggest that the majority of GWAS loci are driven by a single effector gene (Fig. 3b). Next, we wanted to determine how tissue-specific colocalizations were. We grouped xQTL tissues into 32 broad tissue groups (Supplementary Table 3) and found that 44% of associations colocalized with xQTLs from single tissue groups (tissue-specific loci) (Fig. 3c). These findings indicate that PICCOLO can resolve 2,730 (12%) of all genome-wide significant associations to a single gene, and 1,839 (8%) of associations to a single tissue group.

Next, we hypothesized that PICCOLO genes that were specific to trait categories would be enriched for colocalizations in tissues that are biologically relevant. Using the Medical Subject Heading (MeSH) terms we grouped GWAS into 18 trait categories (Supplementary Data 3). For each trait category, we determined the number of PICCOLO genes that were specific or shared across each respective category (Fig. 4a). Blood traits had 1.5× more category specific genes than nonspecific genes ($P = 4.7 \times 10^{-6}$). In contrast, inflammatory traits had 2.2× more nonspecific genes than category specific genes (P = 0.02). While 2,383 (71%) of PICCOLO genes could be attributed to a single trait category, 66 (2%) were highly pleotropic, spanning > 4 trait categories (Fig. 4b, Supplementary Data 4). For each trait category, we tested for the enrichment of xQTL tissues for PICCOLO genes specific to that trait compared to all other PICCOLO colocalizations. Most enriched tissues were clearly biologically relevant. For example, cardiovascular traits were enriched for PICCOLO colocalizations in heart and blood vessel. In contrast, the uterus, vagina, prostate, and pituitary tissue enrichments observed in inflammation traits were less obvious, but biologically insightful (Fig. 4c). The enrichment of colocalizations in sex-specific tissues is consistent with established studies highlighting the strong sex bias and key role of sex hormones in autoimmunity[40-42]. Together, these results demonstrate that PICCOLO identifies genes that are likely specific to one trait category and in biologically relevant tissues.

Next, we tested whether PICCOLO genes were more likely to be disease modulating. For our first analysis, we assessed the enrichment of PICCOLO genes among all genes implicated in rare diseases documented in the Online Mendelian Inheritance in Man (OMIM) Catalog[43] (Supplementary Data 5). Both genes nearest to GWAS associations and non-colocalized genes showed significant 1.2-fold enrichments for OMIM genes ($P = 2.4 \times 10^{-9}$); however, PICCOLO genes were enriched 2.2-fold ($P = 1.4 \times 10^{-12}$, Fig. 5 top). We observed similar enrichments when the analysis was limited to PICCOLO colocalizations with QTLs of a single gene and/or within a single tissue (OR = 2.3, $P = 5.4 \times 10^{-17}$). These data demonstrate that genes identified as influencing complex traits by colocalization are more likely to cause rare disease.

Lastly, we assessed enrichment of PICCOLO genes amongst the target genes of approved drugs in the Pharmaprojects database. Overall, these genes were 2.7-fold enriched ($P = 1.4 \times 10^{-11}$) for successful drug targets, compared to 1.2- and 1.6-fold enrichments for non-colocalized genes and nearest genes respectively (Fig. 5 bottom, Supplementary Fig. 7 and 8). We observed a positive correlation between xQTL –log(P-value) and successful target enrichment which is likely due to the increased confidence in the xQTL and therefore a more robust relationship between gene expression and genotype (Supplementary Fig. 9). Lastly, we found that gene and or tissue specificity of PICCOLO genes resulted in a greater enrichment in both OMIM and Pharmaprojects analyses (Fig. 5), suggesting such evidence may be relevant in assessing a gene's biological relevance.

In summary, we presented a new method that estimates the colocalization between GWAS and xQTL signals without the need for full summary statistics. This innovation greatly expands the number of GWAS and xQTL datasets that can be tested. We observed that xQTLs of colocalized genes tend to be enriched in biologically relevant tissues and enriched for genes linked to rare disease or targets of approved drugs. This work further supports the observations that targets with genetic evidence are more likely to succeed in the clinic[44] and highlights the importance of mapping the correct genes to genetic associations. Our findings also provide motivation for additional xQTL studies in novel cell types.

Together, these data offer the most comprehensive evidence to date that colocalization testing identifies potentially causal genes. As such, we anticipate that PICCOLO and other

colocalization approaches will improve the identification of drug targets from the growing wealth of omic data.

Methods

PICCOLO methodology

PICCOLO is available on github (https://github.com/Ksieber/piccolo) as an R package. This code enables users to download PICS[10] credible sets from the BROAD Institute website (https://pubs.broadinstitute.org/pubs/finemapping/pics.php) and then test two credible sets for colocalization. We removed all credible sets that returned only a single SNP entry from PICS because PICS is unable to differentiate between credible sets with single causal SNPs and SNPs missing from the imputation panel used for the PICs tool. Less than 3% of index SNPs were removed for this reason. The colocalization code is an adaptation from Giambartolomei *et. al*[5]. The default priors are set to be consistent with the default coloc code, where the prior of either genetic signal is 1×10^{-4}, and the prior of two genetic signals being shared is 1×10^{-5}.

xQTLs

Top-hit xQTLs were readily available from sources outlined in Supplementary Table 1. For a given cell type/tissue in each study, we defined the index SNP for each gene as the SNP with the lowest p-value. Using these xQTL index SNPs, we computed the PICS credible sets as outlined in *Farh et al*. (https://pubs.broadinstitute.org/pubs/finemapping/pics.php). Since the cell types and tissues were from multiple sources under different stimuli, we manually grouped cell types into broader categories like those used by the GTEx consortium (Supplementary Table 3).

GWAS

Index SNPs from the NHGRI-EBI GWAS Catalog were downloaded on November 22nd 2017 from https://www.ebi.ac.uk/gwas/downloads. Using these GWAS index SNPs, we computed the PICS credible sets using the same methods used for the xQTL datasets mentioned above. To create a more consistent naming convention for GWAS traits, each trait and was manually mapped to a MeSH term using the MeSH browser, and subsequently assigned to one of 18 trait categories using a similar methodology outlined in Nelson *et al*[44]. Some traits did not match up with a particular MeSH term or category and were classified as “Miscellaneous” (Supplementary Data 3).

Calculating PICCOLO systematically

For every GWAS credible set that we generated, we determined all genes within 500 MB of the index GWAS SNP. For each gene within the 500 kb window, we determined every gene-tissue combination of available xQTL credible sets and calculated the PICCOLO score for every gene-tissue xQTL and GWAS combination.

Calibration with coloc

First, we investigated the distribution of PICCOLO H4 > 0 scores and observed a bimodal distribution (Supplementary Fig. 1). Next, we compared PICCOLO with coloc using a tissue specific approach where the two test results are compared for every trait, in every gene, in every tissue. By evaluating the test statistics of PICCOLO (Supplementary Figure 2), we determined that a PICCOLO cutoff of H4 ≥ 0.9 yields strong predictive power of coloc while maintaining reasonable sensitivity (Supplemental Fig. 2b, positive predictive value = 0.88, true positive rate = 0.45). Given that PICCOLO is estimating many factors, we next asked whether PICCOLO is better at identifying the correct gene at each locus regardless of the tissue specificity. Using this tissue agnostic approach, we observed that PICCOLO H4 ≥ 0.9 was again

ideal and yielded a dramatic improvement in the sensitivity compared to the tissue specific approach (Fig. 2b, Supplementary Fig. 3), positive predictive value = 0.89, true positive rate = 0.52). Lastly, given that PICCOLO is not able to access the uncertainty of the strength of association for the two genetic signals (coloc H0, H1, & H2), we hypothesized that PICCOLO would benefit from titrating eQTL P-value cutoffs. Using the tissue agnostic approach, we determined that a 1×10^{-5} eQTL P-value threshold is ideal predicting coloc results (Supplementary Fig. 3 c, d).

Tissue enrichments

A gene was classified as "shared" if at least 1 eQTL for that gene colocalized with GWAS traits within more than one disease category. To measure the enrichment of tissue groups across each trait category, we first identified all colocalizations with genes that were unique to a single trait category and calculated the proportion of those colocalizations contributed by each tissue. We then calculated the proportion of contribution of each tissue for genes that were shared (i.e. not unique to a single category). Statistical differences in tissue proportion in category specific vs shared genes across tissues was tested using Fisher's exact test (fisher.test) in R.

Gene enrichment for rare diseases and successful drugs

Rare disease genes were downloaded from the OMIM catalog (https://www.omim.org/) accessed June 5th,2018 (Supplementary Data 5). The catalog of successful drug targets was obtained from Pharmaprojects accessed August 5th, 2017 (https://pharmaintelligence.informa.com/products-and-services/data-and-analysis/pharmaprojects) . Each indication was manually mapped MeSH terms and disease categories. Indications that did not fit into a category were annotated as "Miscellaneous". A gene was considered a successful target if there was an approved drug in the United State or European Union that targeted it. Due to the proprietary nature of the gene-indication pairs within the Pharmaproject data, we are unable to share the specific list used here in the supplemental information. However, we included a supplemental table specifying the number of successful drugs per MeSH and the number of targets with PICCOLO evidence. Moreover, we repeated our successful target analysis using the publicly available target-indication data from Nelson *et. al*[44]. and observed nearly identical results (Supplementary Fig. 10).

To test for enrichments, we constructed a 2 × 2 contingency table of genes present in GENCODE (v17) or RefSeq (v37.1). Each box was populated with counts based on the presence or absence of the gene as a successful target (or rare disease gene) versus the presence or absence of a positive PICCOLO colocalization for that gene. Tissue-specific PICCOLO genes were defined as genes within loci where the colocalized xQTLs were all from a single tissue group. Gene-specific PICCOLO genes were defined as genes within loci where only a single gene was colocalized. Tissue and gene specific loci were defined as those within loci where a single gene was colocalized and the corresponding xQTL(s) were from a single tissue group. Odds ratios and 95% confidence intervals calculated using fisher.test in R. Statistical methods used to calculate enrichments are the same as those published in Nelson *et. al*[44].

To determine the percentage of successful trait-indication pairs with evidence of colocalization estimated by PICCOLO, we first selected trait indication-pairs that had an approved drug in the United States or European Union. Next, we removed all target-indication pairs with MeSH terms that did not have at least 1 genome-wide significant association in the GWAS catalog from the analysis (Supplementary Data 6). A target-indication pair was annotated as positive if the target gene matched the colocalized gene and the drug indication was in the same trait category as

the GWAS trait. 95% confidence intervals were calculated using the normal approximation method.

References

1. Visscher, P.M. *et al.* 10 Years of GWAS Discovery: Biology, Function, and Translation. *Am J Hum Genet* **101**, 5-22 (2017).
2. Zhang, F. & Lupski, J.R. Non-coding genetic variants in human disease. *Hum Mol Genet* **24**, R102-10 (2015).
3. Gamazon, E.R. *et al.* Using an atlas of gene regulation across 44 human tissues to inform complex disease- and trait-associated variation. *Nat Genet* **50**, 956-967 (2018).
4. Hormozdiari, F. *et al.* Leveraging molecular quantitative trait loci to understand the genetic architecture of diseases and complex traits. *Nat Genet* **50**, 1041-1047 (2018).
5. Giambartolomei, C. *et al.* Bayesian test for colocalisation between pairs of genetic association studies using summary statistics. *PLoS Genet* **10**, e1004383 (2014).
6. Dobbyn, A. *et al.* Landscape of Conditional eQTL in Dorsolateral Prefrontal Cortex and Co-localization with Schizophrenia GWAS. *Am J Hum Genet* **102**, 1169-1184 (2018).
7. Hauberg, M.E. *et al.* Large-Scale Identification of Common Trait and Disease Variants Affecting Gene Expression. *Am J Hum Genet* **101**, 157 (2017).
8. McLachlan, S. *et al.* Replication and Characterization of Association between ABO SNPs and Red Blood Cell Traits by Meta-Analysis in Europeans. *PLoS One* **11**, e0156914 (2016).
9. Hormozdiari, F. *et al.* Colocalization of GWAS and eQTL Signals Detects Target Genes. *Am J Hum Genet* **99**, 1245-1260 (2016).
10. Farh, K.K. *et al.* Genetic and epigenetic fine mapping of causal autoimmune disease variants. *Nature* **518**, 337-43 (2015).
11. MacArthur, J. *et al.* The new NHGRI-EBI Catalog of published genome-wide association studies (GWAS Catalog). *Nucleic Acids Res* **45**, D896-D901 (2017).
12. Consortium, G.T. Human genomics. The Genotype-Tissue Expression (GTEx) pilot analysis: multitissue gene regulation in humans. *Science* **348**, 648-60 (2015).
13. Lee, M.N. *et al.* Common genetic variants modulate pathogen-sensing responses in human dendritic cells. *Science* **343**, 1246980 (2014).
14. Barreiro, L.B. *et al.* Deciphering the genetic architecture of variation in the immune response to Mycobacterium tuberculosis infection. *Proc Natl Acad Sci U S A* **109**, 1204-9 (2012).
15. Fairfax, B.P. *et al.* Innate immune activity conditions the effect of regulatory variants upon monocyte gene expression. *Science* **343**, 1246949 (2014).
16. Kim-Hellmuth, S. *et al.* Genetic regulatory effects modified by immune activation contribute to autoimmune disease associations. *Nat Commun* **8**, 266 (2017).
17. Ye, C.J. *et al.* Intersection of population variation and autoimmunity genetics in human T cell activation. *Science* **345**, 1254665 (2014).
18. Nedelec, Y. *et al.* Genetic Ancestry and Natural Selection Drive Population Differences in Immune Responses to Pathogens. *Cell* **167**, 657-669 e21 (2016).
19. Caliskan, M., Baker, S.W., Gilad, Y. & Ober, C. Host genetic variation influences gene expression response to rhinovirus infection. *PLoS Genet* **11**, e1005111 (2015).
20. Davenport, E.E. *et al.* Genomic landscape of the individual host response and outcomes in sepsis: a prospective cohort study. *Lancet Respir Med* **4**, 259-71 (2016).
21. Quach, H. *et al.* Genetic Adaptation and Neandertal Admixture Shaped the Immune System of Human Populations. *Cell* **167**, 643-656 e17 (2016).
22. Franco, L.M. *et al.* Integrative genomic analysis of the human immune response to influenza vaccination. *Elife* **2**, e00299 (2013).
23. Naranbhai, V. *et al.* Genomic modulators of gene expression in human neutrophils. *Nat Commun* **6**, 7545 (2015).

24. Raj, T. *et al.* Polarization of the effects of autoimmune and neurodegenerative risk alleles in leukocytes. *Science* **344**, 519-23 (2014).
25. Ferraro, A. *et al.* Interindividual variation in human T regulatory cells. *Proc Natl Acad Sci U S A* **111**, E1111-20 (2014).
26. Fairfax, B.P. *et al.* Genetics of gene expression in primary immune cells identifies cell type-specific master regulators and roles of HLA alleles. *Nat Genet* **44**, 502-10 (2012).
27. Kasela, S. *et al.* Pathogenic implications for autoimmune mechanisms derived by comparative eQTL analysis of CD4+ versus CD8+ T cells. *PLoS Genet* **13**, e1006643 (2017).
28. Westra, H.J. *et al.* Systematic identification of trans eQTLs as putative drivers of known disease associations. *Nat Genet* **45**, 1238-1243 (2013).
29. Zhernakova, D.V. *et al.* Identification of context-dependent expression quantitative trait loci in whole blood. *Nat Genet* **49**, 139-145 (2017).
30. Hao, K. *et al.* Lung eQTLs to help reveal the molecular underpinnings of asthma. *PLoS Genet* **8**, e1003029 (2012).
31. Qiu, W. *et al.* Genetics of sputum gene expression in chronic obstructive pulmonary disease. *PLoS One* **6**, e24395 (2011).
32. Parisien, M. *et al.* Effect of Human Genetic Variability on Gene Expression in Dorsal Root Ganglia and Association with Pain Phenotypes. *Cell Rep* **19**, 1940-1952 (2017).
33. Schadt, E.E. *et al.* Mapping the genetic architecture of gene expression in human liver. *PLoS Biol* **6**, e107 (2008).
34. Innocenti, F. *et al.* Identification, replication, and functional fine-mapping of expression quantitative trait loci in primary human liver tissue. *PLoS Genet* **7**, e1002078 (2011).
35. Suhre, K. *et al.* Connecting genetic risk to disease end points through the human blood plasma proteome. *Nat Commun* **8**, 14357 (2017).
36. Sun, B.B. *et al.* Genomic atlas of the human plasma proteome. *Nature* **558**, 73-79 (2018).
37. Varshney, A. *et al.* Genetic regulatory signatures underlying islet gene expression and type 2 diabetes. *Proc Natl Acad Sci U S A* **114**, 2301-2306 (2017).
38. Ko, Y.A. *et al.* Genetic-Variation-Driven Gene-Expression Changes Highlight Genes with Important Functions for Kidney Disease. *Am J Hum Genet* **100**, 940-953 (2017).
39. Elliott, L. *et al.* Genome-wide association studies of brain structure and function in the UK Biobank. *bioRxiv* (2018).
40. Trigunaite, A., Dimo, J. & Jorgensen, T.N. Suppressive effects of androgens on the immune system. *Cell Immunol* **294**, 87-94 (2015).
41. Rubtsova, K., Marrack, P. & Rubtsov, A.V. Sexual dimorphism in autoimmunity. *J Clin Invest* **125**, 2187-93 (2015).
42. Wilhelmson, A.S. *et al.* Testosterone is an endogenous regulator of BAFF and splenic B cell number. *Nat Commun* **9**, 2067 (2018).
43. Online Mendelian Inheritance in Man, OMIM. Vol. 2017 (McKusick-Nathans Institute of Genetic Medicine, Johns Hopkins University (Baltimore, MD)).
44. Nelson, M.R. *et al.* The support of human genetic evidence for approved drug indications. *Nat Genet* **47**, 856-60 (2015).

Figures

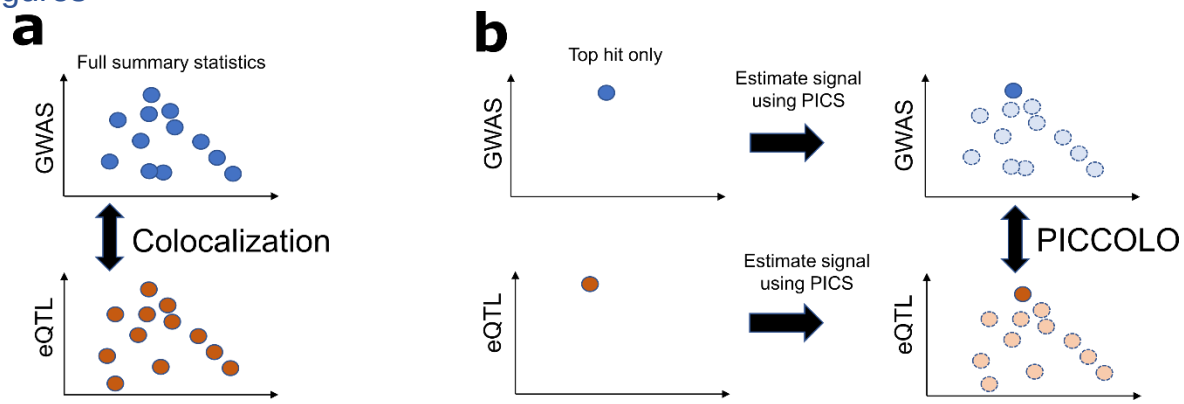

Figure 1: Colocalization of genetic signals using PICCOLO.

(a) Colocalization requires full summary statistics from both the GWAS and xQTL studies. **(b)** PICCOLO uses association top hits and estimates the "missing" data using PICS. The PICS sets are then colocalized using the *coloc* method.

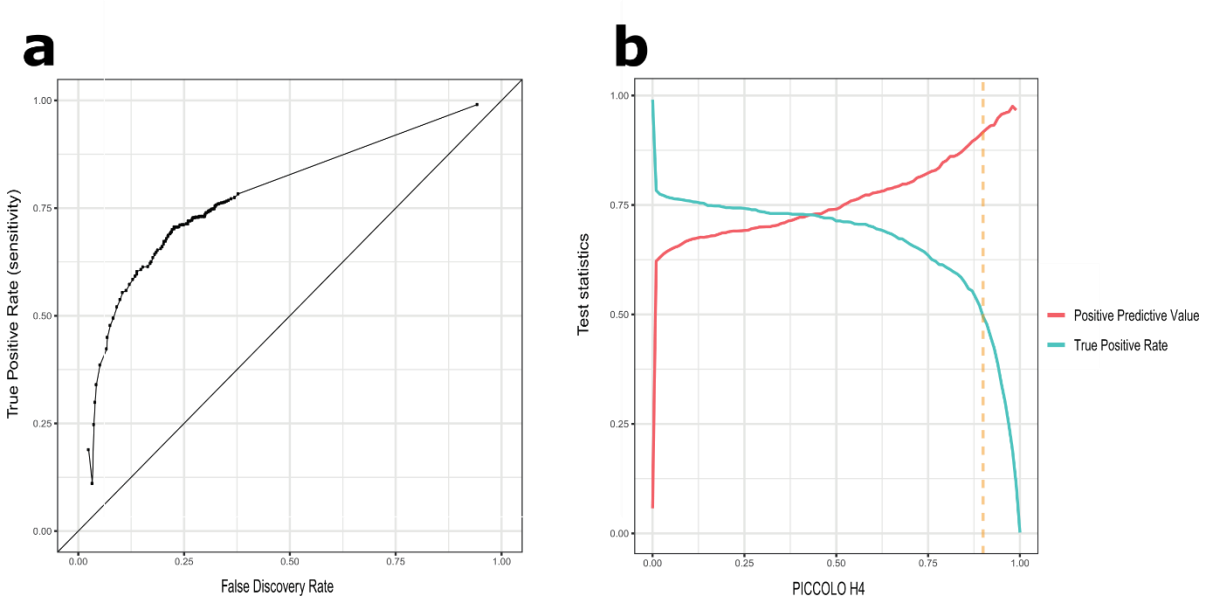

Figure 2: Calibration of PICCOLO with coloc

Using index SNPs, PICCOLO was evaluated for the ability to predict colocalization (coloc H4 ≥ 0.80). **(a)** ROC comparing PICCOLO to coloc in a tissue agnostic manner. **(b)** Using the balanced PICCOLO parameters (orange dashed line, H4 ≥ 0.90 and an xQTL P ≤ 1×10^{-5}), PICCOLO has a positive predictive value (red line) of 0.89 and sensitivity (blue line) of 0.52 for coloc (coloc H4 ≥ 0.8).

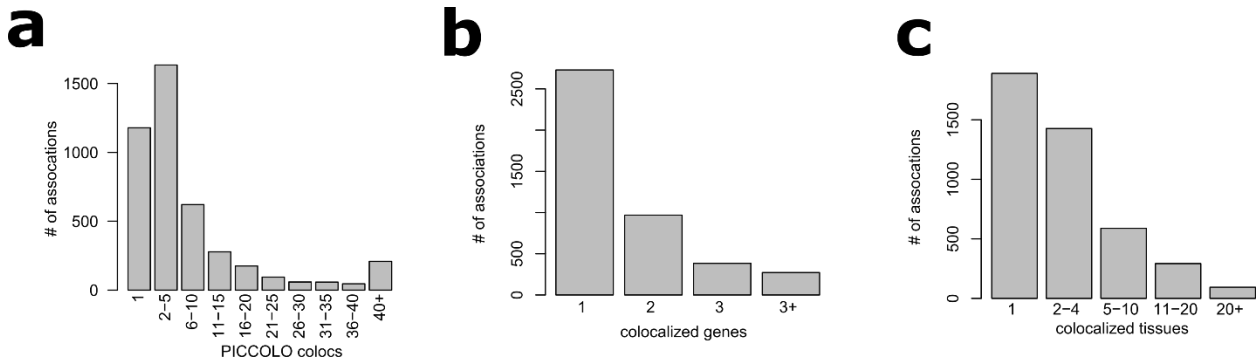

Figure 3: Colocalization of the NHGRI-EBI GWAS Catalog with xQTLs using PICCOLO.
(a) Distribution of the number of colocalizations (tissue-gene pairs) at each GWAS association. **(b)** Distribution of the number of PICCOLO genes at each association. **(c)** Distribution of the number of tissue groups with colocalizations at each GWAS association.

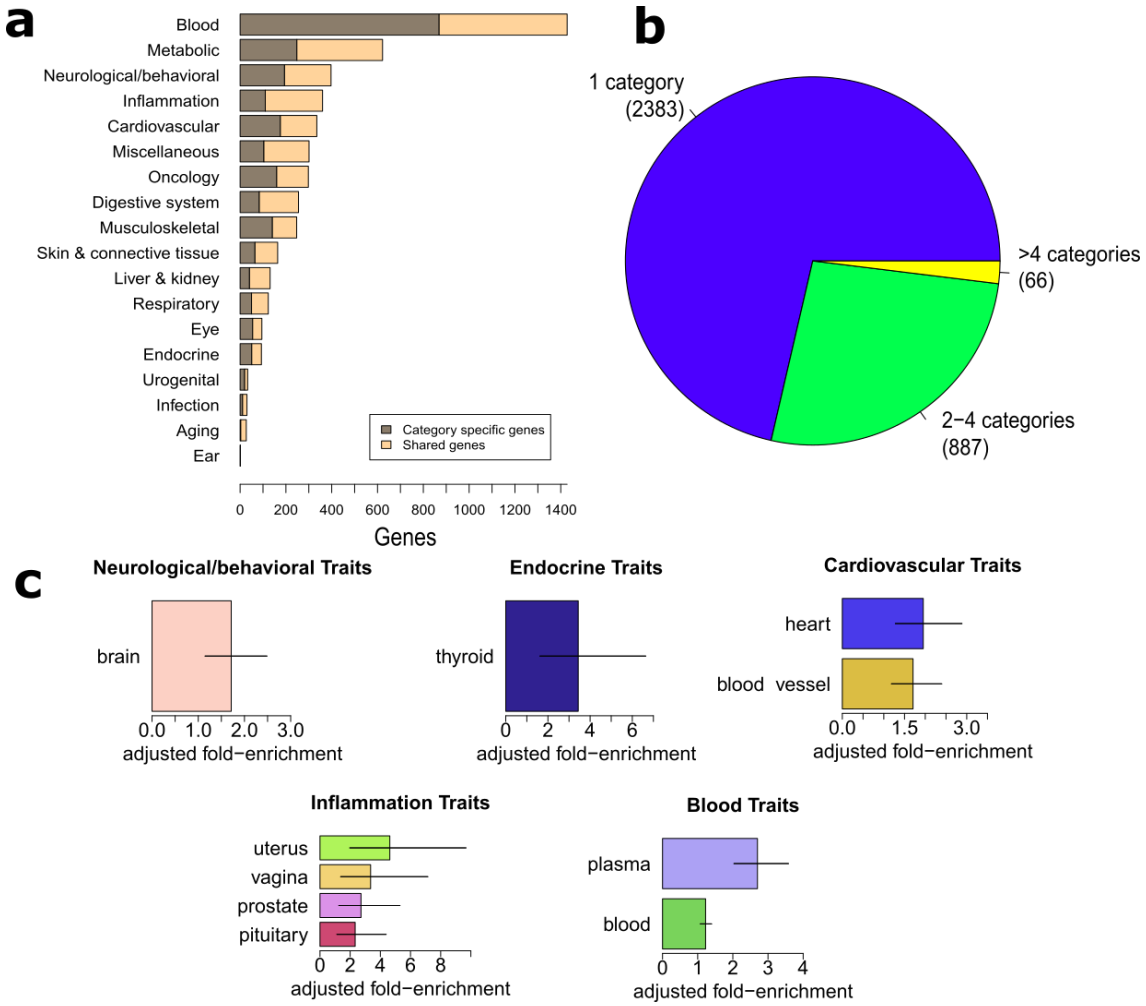

Figure 4: PICCOLO results across different trait categories.

(a) Number of PICCOLO genes that are shared across one or more trait categories (beige) and number of PICCOLO genes that are specific to a trait category (grey). **(b)** Proportion of PICCOLO genes that map to a single therapy category (blue), 2-4 categories (green), and >4 categories (yellow). **(c)** Enrichment of QTL tissues for trait category specific PICCOLO genes across neurological/behavioral, endocrine, cardiovascular, inflammation, and blood-related traits. Bars show 95% confidence intervals. All enrichments are significant at an FDR of 0.5. If a trait category or tissue is not shown, it means that the category specific genes were not enriched for PICCOLO genes that colocalize in those tissues.

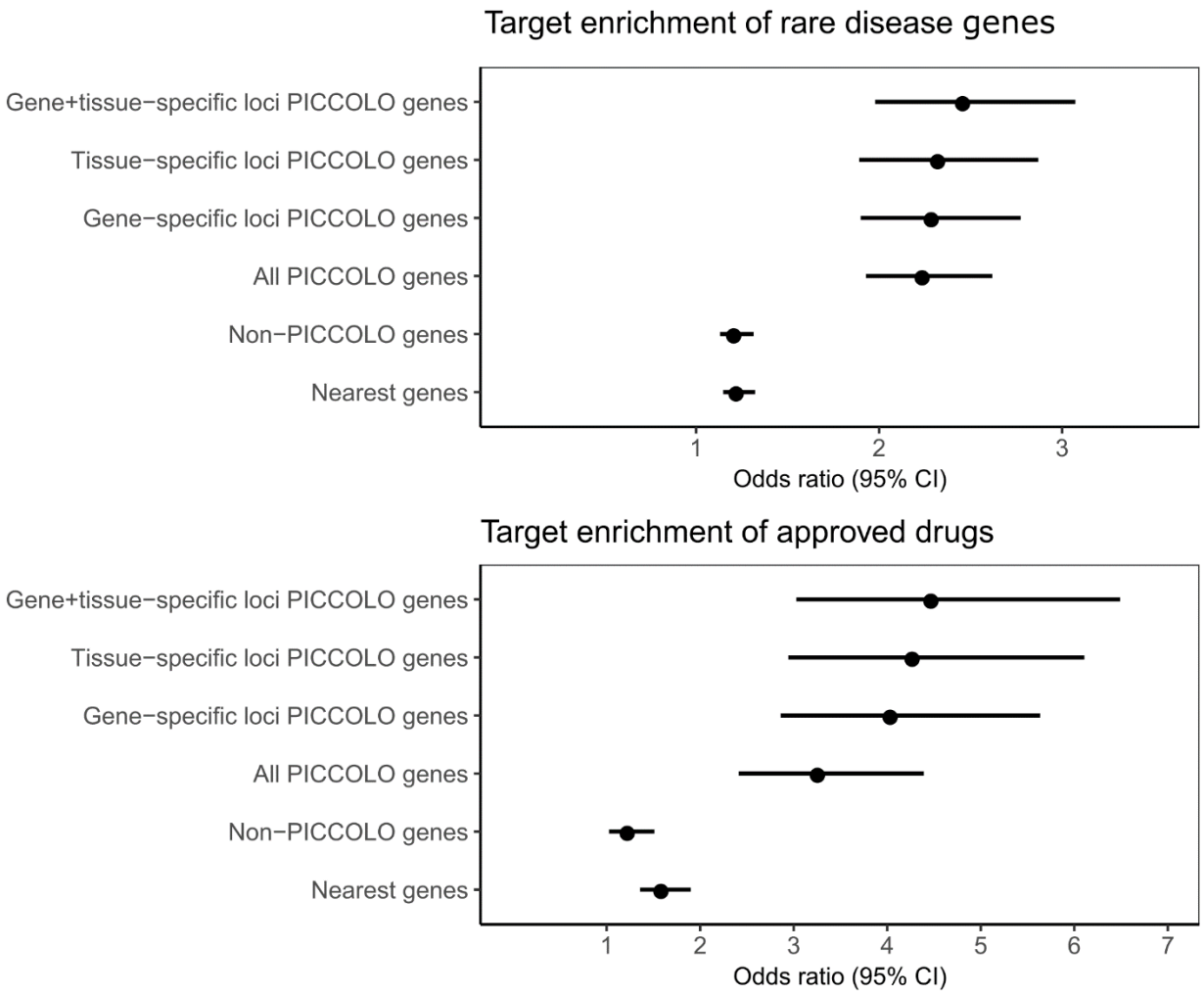

Figure 5: Enrichment of rare disease genes, approved drug targets and overlap between drug targets and PICCOLO genes.

Enrichments for rare disease genes in OMIM (top), and approved drug targets in the United States and the European Union (bottom). Enrichment was tested for genes nearest to GWAS index SNPs (Nearest genes), genes that were found to not be colocalized using PICCOLO (Non-PICCOLO genes), all genes found to be colocalized using PICCOLO (All PICCOLO genes), PICCOLO genes within loci where only one gene is colocalized (Gene-specific loci PICCOLO genes), genes within loci where colocalization occur in a single tissue (Tissue-specific loci PICCOLO genes), and PICCOLO genes within loci where a single gene is colocalized in a single tissue (Gene+tissue-specific loci PICCOLO genes). Bars show 95% confidence intervals.

Supplementary Figures

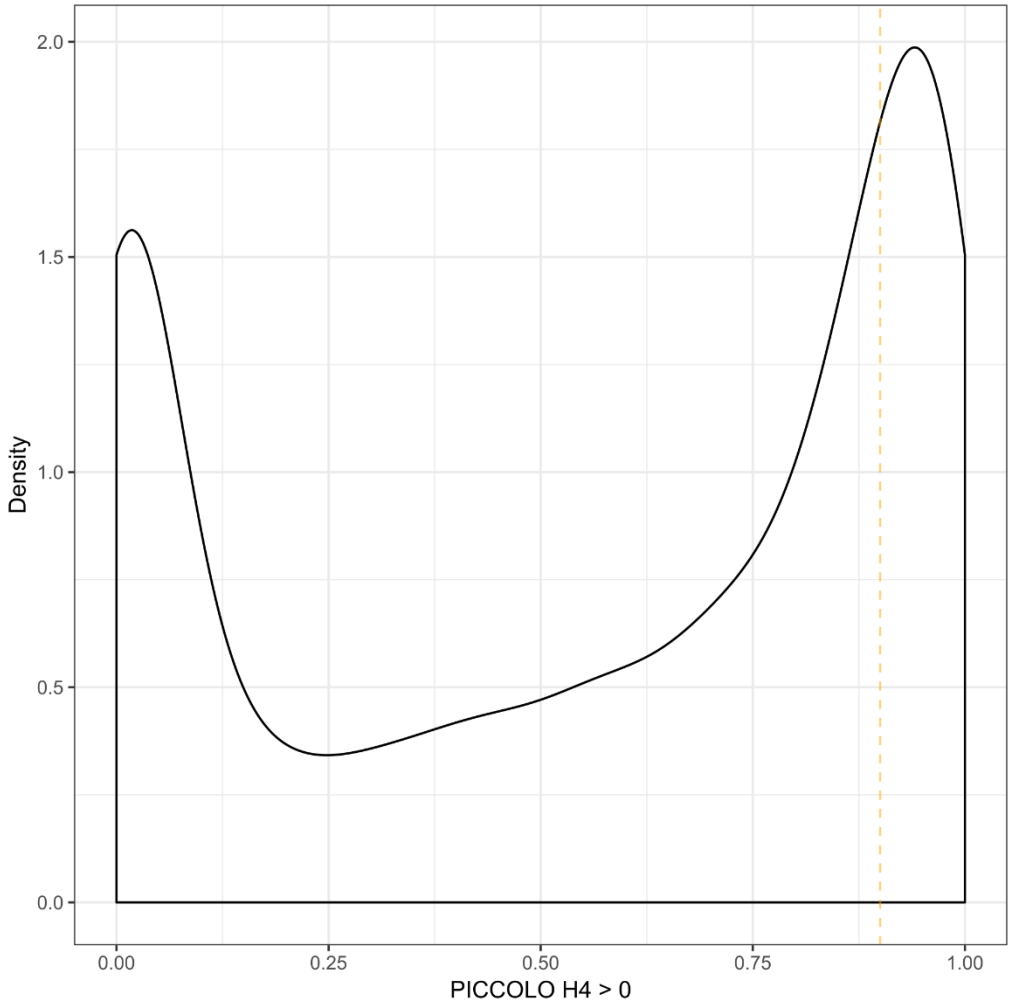

Supplementary Figure 1: PICCOLO H4 Distribution

Distribution of non-zero PICCOLO H4 scores for associations with 13 traits from the Elliot *et. al.* analysis of the UKBiobank[39] colocalized with GTEx.

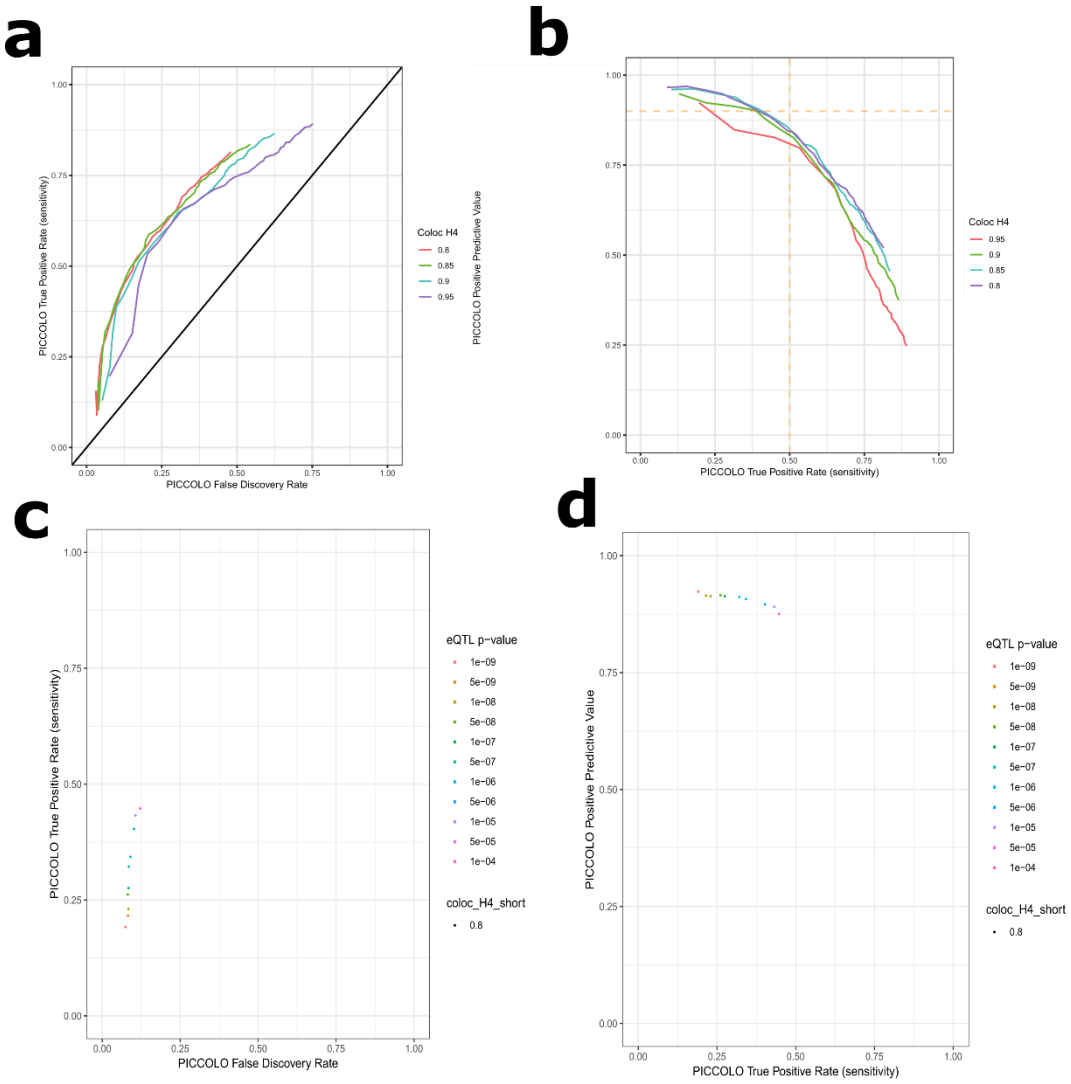

Supplementary Figure 2: PICCOLO sensitivity tissue specific

(a) Using the tissue specific approach, a ROC compares the sensitivity (y-axis) to the false discovery rate (x-axis) of PICCOLO predicting colocalization at multiple coloc H4 thresholds (colored lines). **(b)** The positive predictive value (y-axis) compared the true positive rate (x-axis) of PICCOLO predicting colocalization across multiple coloc H4 thresholds (colored lines). Similar to panels (a) and (b), panels **(c)** and **(d)** compare the same test statistics, respectively, while holding the PICCOLO H4 (0.9) and coloc H4 (0.8) constant while titrating the xQTL P-values (colored dots).

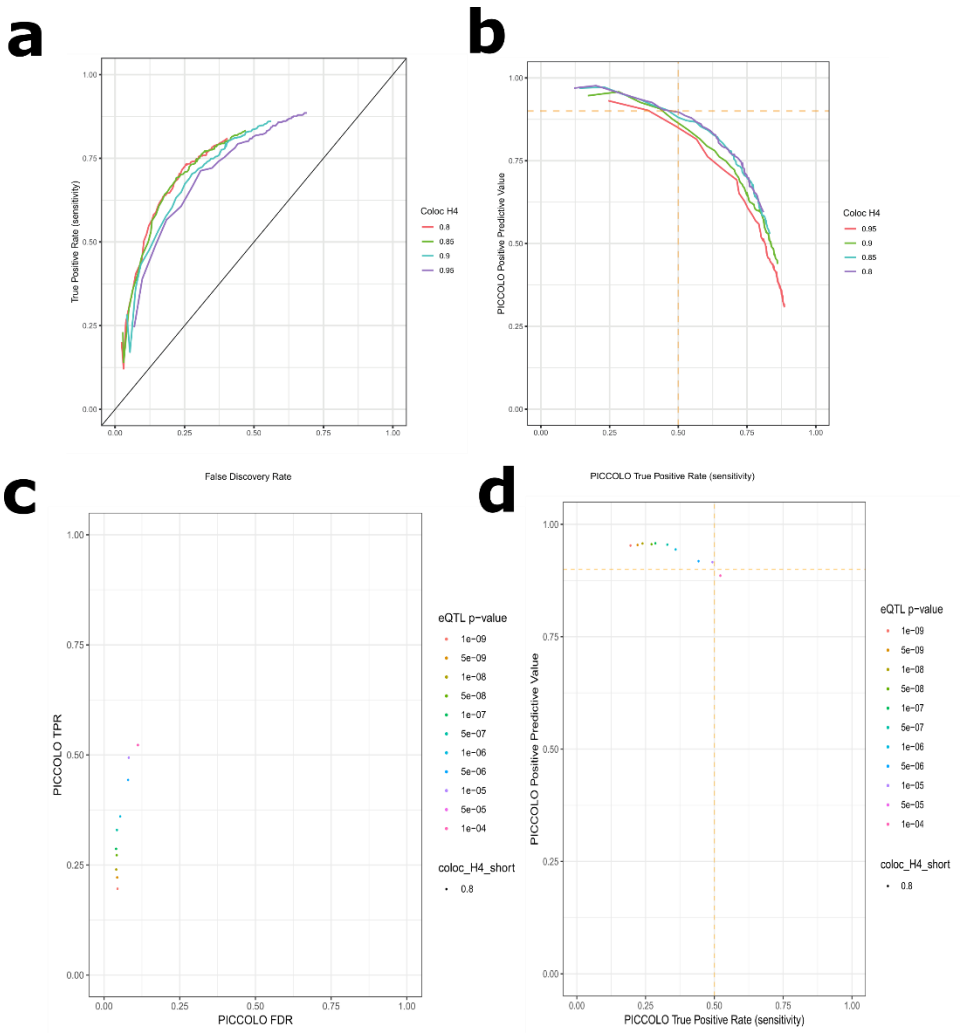

Supplementary Figure 3: PICCOLO sensitivity tissue agnostic

(a) Using the tissue agnostic approach, a ROC compares the sensitivity (y-axis) to the false discovery rate (x-axis) of PICCOLO predicting colocalization at multiple coloc H4 thresholds (colored lines). **(b)** The positive predictive value (y-axis) compared the true positive rate (x-axis) of PICCOLO predicting colocalization across multiple coloc H4 thresholds (colored lines). Similar to panels (a) and (b), panels **(c)** and **(d)** compare the same test statistics, respectively, while holding the PICCOLO H4 (0.9) and coloc H4 (0.8) constant while titrating the xQTL P-values (colored dots).

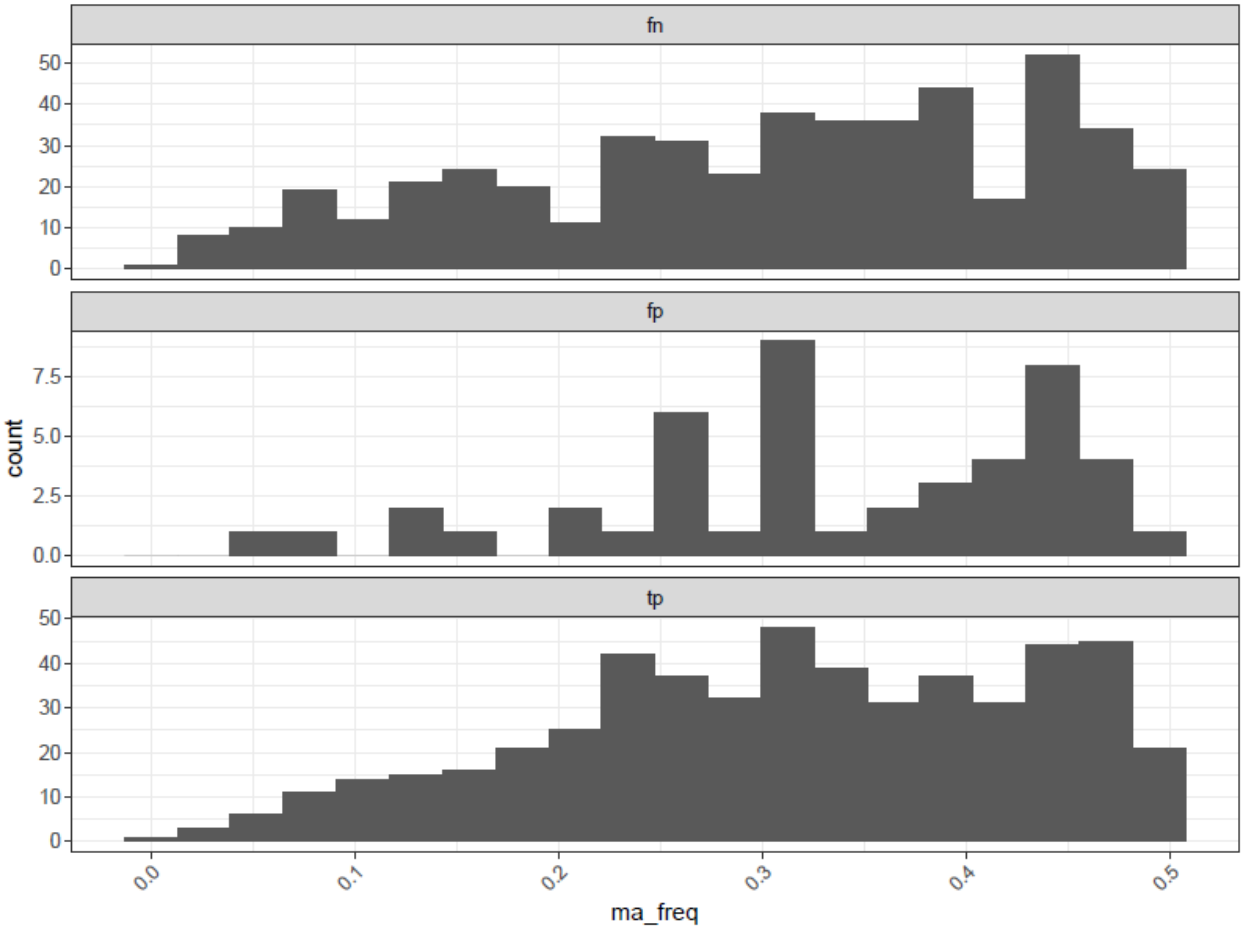

Supplementary Figure 4: The distribution of the tested GWAS minor allele frequency index SNPs used to compare PICCOLO and coloc.

Using the PICCOLO and coloc comparison dataset, PICCOLO results were determined to be either false negatives (fn, top), false positives (fp, mid), or true positives (tp, bottom) based on the results of coloc (H4 ≥ 0.80). For each category, the distribution (y-axis) of the minor allele frequency (x-axis) of the GWAS index SNP is plotted.

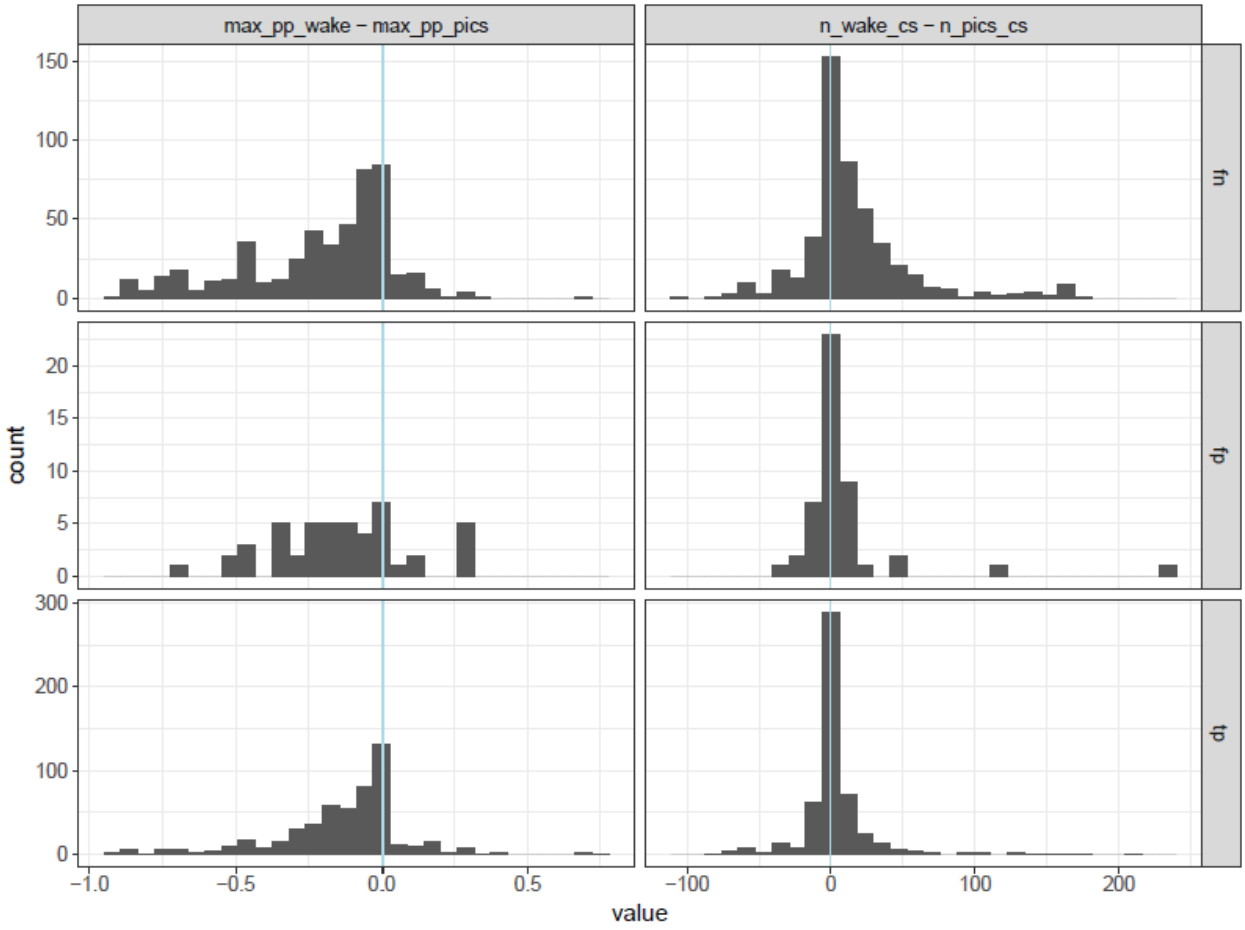

Supplementary Figure 5: Comparison of the Wakefield and PICS GWAS credible set size and max posterior probability.

Using the PICCOLO and coloc comparison dataset, PICCOLO results were determined to be either false negatives (fn, top), false positives (fp, mid), or true positives (tp, bottom) based on the results of coloc (H4 ≥ 0.80). For each category, the distributions of the difference between Wakefield (used for coloc) and the PICs max posterior probability (left panels) and number of SNPs (right panels) for each GWAS credible set are plotted. The vertical blue line illustrates the count where there were no differences between the two methods.

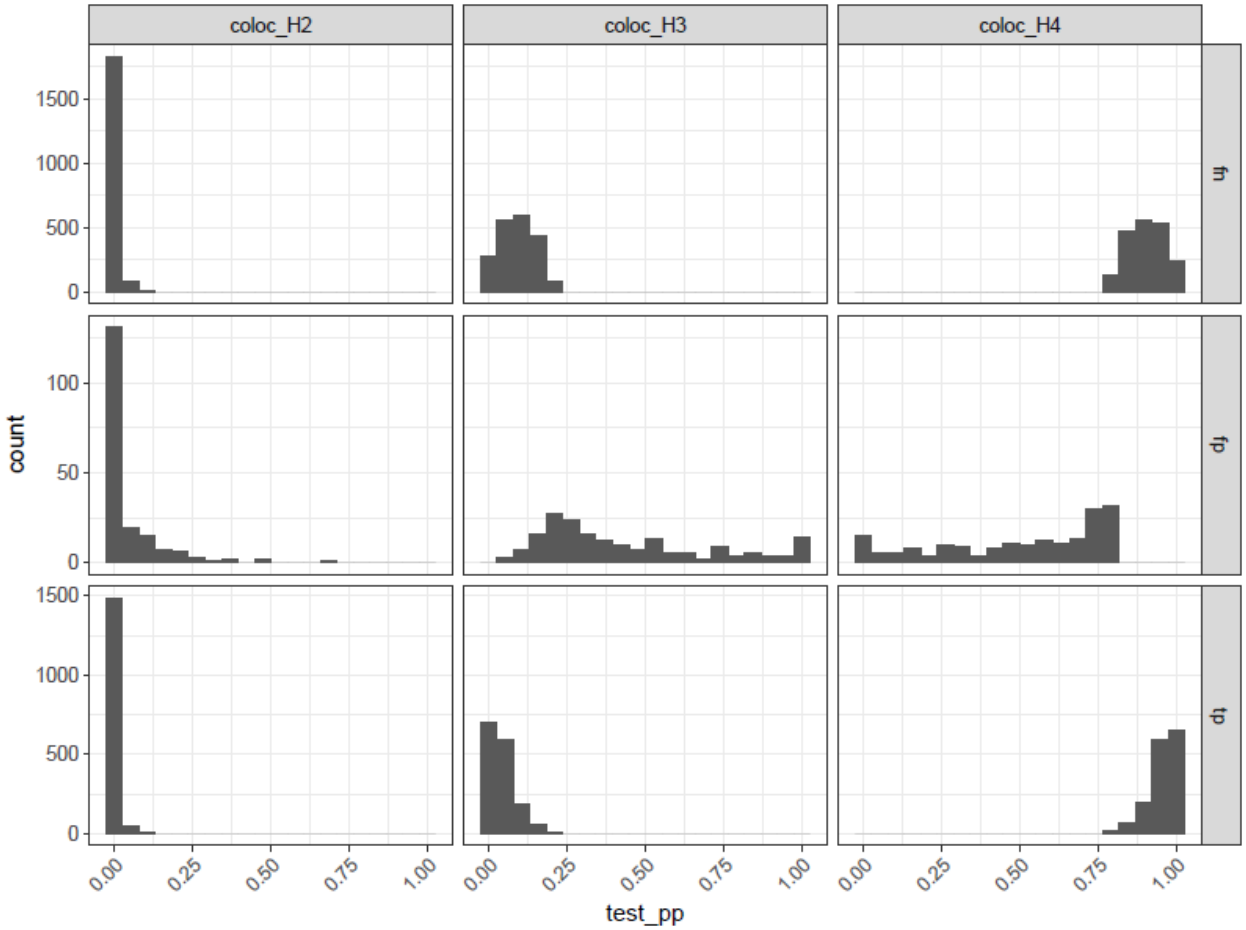

Supplementary Figure 6: distribution of differences in H2, H3, and H4 for false positives, and true positives

Using the PICCOLO and coloc comparison dataset, PICCOLO results were determined to be either false negatives (fn, top), false positives (fp, mid), or true positives (tp, bottom) based on the results of coloc (H4 ≥ 0.80). For each category, the distribution (y-axis) of the alternative coloc hypotheses test posterior probabilities (x-axis, test_pp) are plotted.

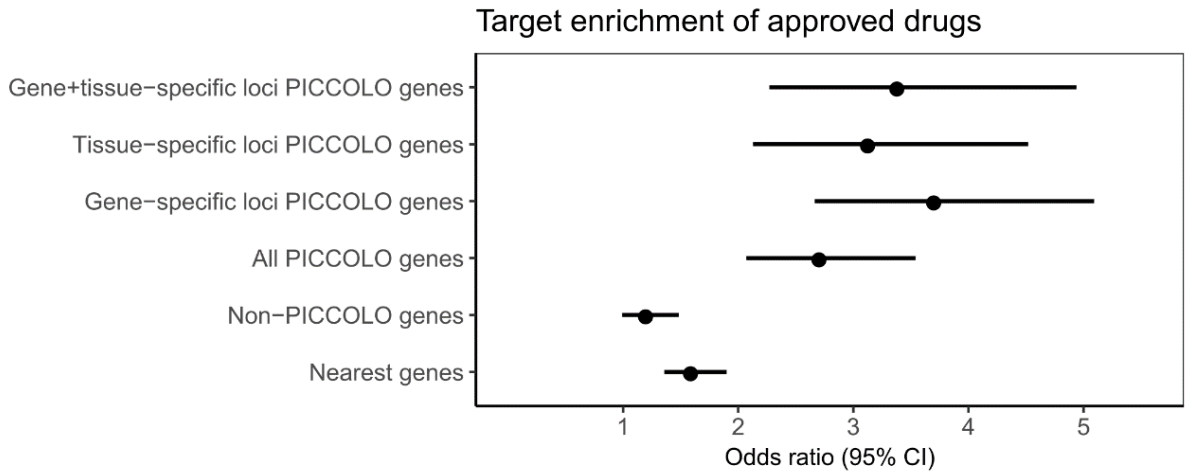

Supplementary Figure 7: Enrichment of approved drug targets using a PICCOLO H4 ≥ 0.9 and an QTL P ≤ 1 × 10-5

Enrichment was is tested for genes nearest to GWAS index SNPs (Nearest genes), genes that were found to not be colocalized using PICCOLO (Non-PICCOLO genes), all genes found to be colocalized using PICCOLO (All PICCOLO genes), PICCOLO genes within loci where only one gene is colocalized (Gene-specific loci PICCOLO genes), genes within loci where colocalization occur in a single tissue (Tissue-specific loci PICCOLO genes), and PICCOLO genes within loci where a single gene is colocalized in a single tissue (Gene+tissue-specific loci PICCOLO genes). Bars show 95% confidence intervals.

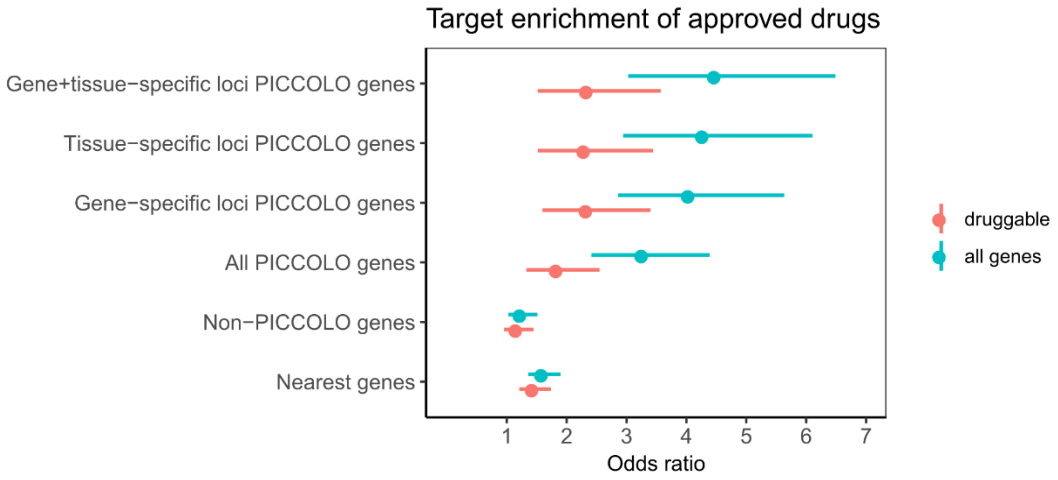

Supplementary Figure 8: Enrichment of approved drug targets for all genes and the druggable genome.

PICCOLO gene enrichment for approved drug targets compared to all protein coding genes in the genome (blue) and all druggable genes (red). Enrichment was is tested for genes nearest to GWAS index SNPs (Nearest genes), genes that were found to not be colocalized using PICCOLO (Non-PICCOLO genes), all genes found to be colocalized using PICCOLO (All PICCOLO genes), PICCOLO genes within loci where only one gene is colocalized (Gene-specific loci PICCOLO genes), genes within loci where colocalization occur in a single tissue (Tissue-specific loci PICCOLO genes), and PICCOLO genes within loci where a single gene is colocalized in a single tissue (Gene+tissue-specific loci PICCOLO genes). Bars show 95% confidence intervals.

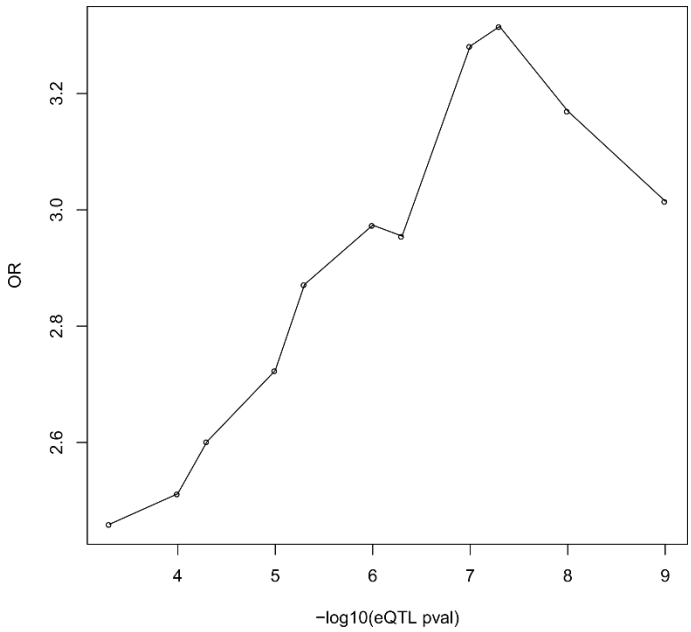

Supplementary Figure 9: Enrichment of approved drug targets in relation to xQTL P-value cutoff

Points show the mean PICCOLO gene enrichment at xQTL $-\log_{10}$(P-value cutoff) (x-axis).

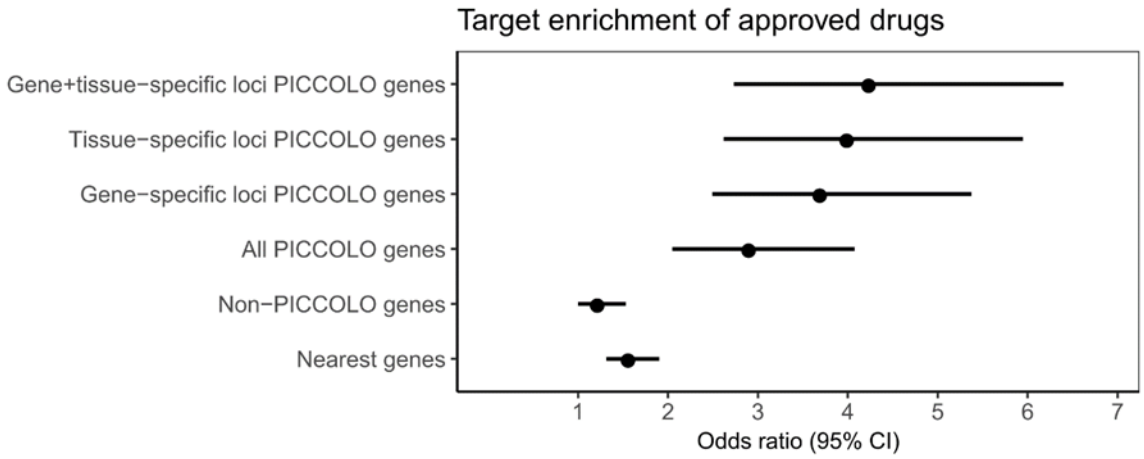

Supplementary Figure 10: Enrichment of approved drug targets using the Nelson et. al. 2015 successful target-indication pairs dataset.

Enrichment was is tested for genes nearest to GWAS index SNPs (Nearest genes), genes that were found to not be colocalized using PICCOLO (Non-PICCOLO genes), all genes found to be colocalized using PICCOLO (All PICCOLO genes), PICCOLO genes within loci where only one gene is colocalized (Gene-specific loci PICCOLO genes), genes within loci where colocalization occur in a single tissue (Tissue-specific loci PICCOLO genes), and PICCOLO genes within loci where a single gene is colocalized in a single tissue (Gene+tissue-specific loci PICCOLO genes). Bars show 95% confidence intervals.

Supplementary Tables

Supplementary Table 1: QTLs sources used in PICCOLO analyses

First Author	PMID	TISSUE	QTL type
GTEx	29022597	Multi	eQTL
Lee	24604203	Dendritic cells (derived from monocytes)	eQTL
Barreiro	22233810	Dendritic cells	eQTL
Fairfax	24604202	Monocytes	eQTL
Kim-Hellmuth	28814792	Monocytes	eQTL
Ye	25214635	CD4+ T cells	eQTL
Nédélec	27768889	Monocyte derived Macrophage	eQTL
Çalışkan	25874939	PBMCs	eQTL
Davenport	26917434	Leucocytes	eQTL
Quach	27768888	Monocytes	eQTL
Franco	23878721	Whole blood	eQTL
Naranbhai	26151758	Neutrophils	eQTL
Raj	24786080	CD4(+) T cells and monocytes	eQTL
Ferraro	24610777	CD4(+) T cells and T regs	eQTL
Fairfax	22446964	monocytes and B-cells	eQTL
Kasela	28248954	CD4+ and CD8+ T cells	eQTL
Westra	24013639	whole blood	eQTL
Zhernakova	27918533	whole blood	eQTL
Hao	23209423	lung	eQTL
Qui	21949713	sputum from COPD patients (ECLIPSE)	pQTL
Parisien	28564610	Dorsal Root Ganglion	eQTL
UBIOPRED	NA	Serum from asthma patients	pQTL
Schadt	18462017	Liver	eQTL
Innocenti	21637794	Liver	eQTL
Suhre	28240269	plasma	pQTL
Sun	29875488	plasma	pQTL
Varshney	28193859	islet	eQTL
Ko	28575649	kidney	eQTL

Supplementary Table 2: GWAS used for comparison between coloc and PICCOLO

Analysis	Description	ncase	ncohort
neale17_1239	Current tobacco smoking (UKB Broad)	NA	337030
neale17_1558	Alcohol intake frequency. (UKB Broad)	NA	336965
neale17_20002_1111	Non-cancer illness code, self-reported: asthma (UKB Broad)	39049	NA
neale17_20002_1112	Non-cancer illness code, self-reported: chronic obstructive airways disease/copd (UKB Broad)	1179	NA
neale17_20002_1473	Non-cancer illness code, self-reported: high cholesterol (UKB Broad)	41296	NA
neale17_2090	Seen doctor (GP) for nerves, anxiety, tension or depression (UKB Broad)	115328	NA
neale17_21001	Body mass index (BMI) (UKB Broad)	NA	336107
neale17_47	Hand grip strength (right) (UKB Broad)	NA	335842
neale17_50	Standing height (UKB Broad)	NA	336474
neale17_6150_4	Vascular/heart problems diagnosed by doctor: High blood pressure (UKB Broad)	91033	NA
neale17_6159_4	Pain type(s) experienced in last month: Back pain (UKB Broad)	85221	NA
neale17_78	Heel bone mineral density (BMD) T-score, automated (UKB Broad)	NA	194398
neale17_I25	Diagnoses - main ICD10: I25 Chronic ischemic heart disease (UKB Broad)	8755	NA

Supplementary Table 3: Tissue grouping key for xQTL studies

Tissue group	Tissue type	Cell type
blood	b-cell	B-cell
blood	t-cell	CD4
blood	t-cell	CD4-cis-allconditions
blood	t-cell	CD4-meta-cis
blood	dendritic	Dendritic-cells-Flu
blood	dendritic	Dendritic-cells-IFNb
blood	dendritic	Dendritic-cells-LPS
blood	dendritic	Dendritic-cells-naive
blood	dendritic	Dendritic-cells-re-Flu
blood	dendritic	Dendritic-cells-re-IFNb
blood	dendritic	Dendritic-cells-re-LPS
blood	dendritic	Dendritic-MTB
blood	dendritic	Dendritic-naive
blood	dendritic	Dendritic-re-MTB
lung	Epithelium-airway-cis	Epithelium-airway-cis
lung	Epithelium-airway-trans	Epithelium-airway-trans
adipose_tissue	gtex-v6p-adipose-subcutaneous	gtex-v6p-adipose-subcutaneous
adipose_tissue	gtex-v6p-adipose-visceral-omentum	gtex-v6p-adipose-visceral-omentum
adrenal_gland	gtex-v6p-adrenal-gland	gtex-v6p-adrenal-gland
blood_vessel	gtex-v6p-artery-aorta	gtex-v6p-artery-aorta
blood_vessel	gtex-v6p-artery-coronary	gtex-v6p-artery-coronary
blood_vessel	gtex-v6p-artery-tibial	gtex-v6p-artery-tibial
bladder	gtex-v6p-bladder	gtex-v6p-bladder
brain	gtex-v6p-brain-amygdala	gtex-v6p-brain-amygdala
brain	gtex-v6p-brain-anterior-cingulate-cortex-ba24	gtex-v6p-brain-anterior-cingulate-cortex-ba24
brain	gtex-v6p-brain-caudate-basal-ganglia	gtex-v6p-brain-caudate-basal-ganglia
brain	gtex-v6p-brain-cerebellar-hemisphere	gtex-v6p-brain-cerebellar-hemisphere
brain	gtex-v6p-brain-cerebellum	gtex-v6p-brain-cerebellum
brain	gtex-v6p-brain-cortex	gtex-v6p-brain-cortex
brain	gtex-v6p-brain-frontal-cortex-ba9	gtex-v6p-brain-frontal-cortex-ba9
brain	gtex-v6p-brain-hippocampus	gtex-v6p-brain-hippocampus
brain	gtex-v6p-brain-hypothalamus	gtex-v6p-brain-hypothalamus
brain	gtex-v6p-brain-nucleus-accumbens-basal-ganglia	gtex-v6p-brain-nucleus-accumbens-basal-ganglia
brain	gtex-v6p-brain-putamen-basal-ganglia	gtex-v6p-brain-putamen-basal-ganglia
brain	gtex-v6p-brain-spinal-cord-cervical-c-1	gtex-v6p-brain-spinal-cord-cervical-c-1
brain	gtex-v6p-brain-substantia-nigra	gtex-v6p-brain-substantia-nigra
breast	gtex-v6p-breast-mammary-tissue	gtex-v6p-breast-mammary-tissue
blood	b-cell	gtex-v6p-cells-ebv-transformed-lymphocytes
skin	gtex-v6p-cells-transformed-fibroblasts	gtex-v6p-cells-transformed-fibroblasts
cervix_uteri	gtex-v6p-cervix-ectocervix	gtex-v6p-cervix-ectocervix
cervix_uteri	gtex-v6p-cervix-endocervix	gtex-v6p-cervix-endocervix
colon	gtex-v6p-colon-sigmoid	gtex-v6p-colon-sigmoid
colon	gtex-v6p-colon-transverse	gtex-v6p-colon-transverse
esophagus	gtex-v6p-esophagus-gastroesophageal-junction	gtex-v6p-esophagus-gastroesophageal-junction
esophagus	gtex-v6p-esophagus-mucosa	gtex-v6p-esophagus-mucosa
esophagus	gtex-v6p-esophagus-muscularis	gtex-v6p-esophagus-muscularis
fallopian_tube	gtex-v6p-fallopian-tube	gtex-v6p-fallopian-tube
heart	gtex-v6p-heart-atrial-appendage	gtex-v6p-heart-atrial-appendage
heart	gtex-v6p-heart-left-ventricle	gtex-v6p-heart-left-ventricle
kidney	gtex-v6p-kidney-cortex	gtex-v6p-kidney-cortex
liver	gtex-v6p-liver	gtex-v6p-liver
lung	Lung	gtex-v6p-lung
salivary_gland	gtex-v6p-minor-salivary-gland	gtex-v6p-minor-salivary-gland
muscle	gtex-v6p-muscle-skeletal	gtex-v6p-muscle-skeletal
nerve	gtex-v6p-nerve-tibial	gtex-v6p-nerve-tibial
ovary	gtex-v6p-ovary	gtex-v6p-ovary
pancreas	gtex-v6p-pancreas	gtex-v6p-pancreas
pituitary	gtex-v6p-pituitary	gtex-v6p-pituitary
prostate	gtex-v6p-prostate	gtex-v6p-prostate
skin	gtex-v6p-skin-not-sun-exposed-suprapubic	gtex-v6p-skin-not-sun-exposed-suprapubic
skin	gtex-v6p-skin-sun-exposed-lower-leg	gtex-v6p-skin-sun-exposed-lower-leg
small_intestine	gtex-v6p-small-intestine-terminal-ileum	gtex-v6p-small-intestine-terminal-ileum
spleen	gtex-v6p-spleen	gtex-v6p-spleen
stomach	gtex-v6p-stomach	gtex-v6p-stomach

testis	gtex-v6p-testis	gtex-v6p-testis
thyroid	gtex-v6p-thyroid	gtex-v6p-thyroid
uterus	gtex-v6p-uterus	gtex-v6p-uterus
vagina	gtex-v6p-vagina	gtex-v6p-vagina
blood	blood	gtex-v6p-whole-blood
liver	hepatocytes	HLC
ipsc	ipsc	IPSC
pancreas	islet	Islet
kidney	kidney	Kidney
blood	leukocyte	Leuco-sepsis
liver	liver	Liver
lung	lung	Lung-cis
blood	macrophage	Macro-Listeria
blood	macrophage	Macro-naive
blood	macrophage	Macro-re-Listeria
blood	macrophage	Macro-re-Salmonella
blood	macrophage	Macro-Salmonella
blood	monocyte	Mono
blood	monocyte	Monocyte
blood	monocyte	Mono-Flu
blood	monocyte	Mono-IFN
blood	monocyte	Mono-LPS
blood	monocyte	Mono-LPS-24h
blood	monocyte	Mono-LPS-2h
blood	monocyte	Mono-LPS-6h
blood	monocyte	Mono-LPS-90m
blood	monocyte	Mono-mdp-6h
blood	monocyte	Mono-mdp-90m
blood	monocyte	Mono-naive
blood	monocyte	Mono-Pam3CSK4
blood	monocyte	Mono-R848
blood	monocyte	Mono-re-Flu
blood	monocyte	Mono-re-LPS
blood	monocyte	Mono-re-LPS-6h
blood	monocyte	Mono-re-LPS-90m
blood	monocyte	Mono-re-mdp-6h
blood	monocyte	Mono-re-mdp-90m
blood	monocyte	Mono-re-Pam3CSK4
blood	monocyte	Mono-re-R848
blood	monocyte	Mono-re-rna-6h
blood	monocyte	Mono-re-rna-90m
blood	monocyte	Mono-rna-6h
blood	monocyte	Mono-rna-90min
blood	neutrophil	Neutro
blood	blood	PBMC-naive
blood	blood	PBMC-re-rv
blood	blood	PBMC-rv
plasma	plasma	Plasma-pQTL
plasma	plasma	Serum-cis-pQTL
plasma	plasma	Serum-pQTL-cis
plasma	plasma	Serum-trans-pQTL
lung	sputum	Sputum-COPD-patients-ECLIPSE-cis
blood	t-cell	Treg
blood	blood	WB-naive

Supplementary Data Sets

Supplementary Data Set 1: PICCOLO and coloc results for 13 traits colocalized with GTEx

Supplementary Data Set 2: All PICCOLO results

Supplementary Data Set 3: GWAS Catalog with MeSH annotations

Supplementary Data Set 4: Number of tissues and diseases per gene

Supplementary Data Set 5: OMIM Genes

Supplementary Data Set 6: Number of associations per MeSH

Supplementary Data Set 7: Number of successful drug targets with PICCOLO evidence by MeSH

Author contributions

C.G. and K.B.S jointly conceptualized the study and lead the analyses. J.E.G. and M.R.H obtained the xQTL datasets and performed the MeSH annotations. T.J. and M.R.N provided scientific guidance and assisted with the analyses. C.G. and K.B.S wrote the manuscript with assistance from all other authors.

Acknowledgements

We would like to thank Meg G. Ehm for her suggestions on the manuscript. We are appreciative of John H. Riley, Stewart A. Bates, and the rest of the U-BIOPRED group for allowing us to use their unpublished pQTL results.

Competing interests

All authors are employees of GlaxoSmithKline.